WARSAW UNIVERSITY OF TECHNOLOGY Index 351733
FACULTY OF CIVIL ENGINEERING
COMMITTEE FOR CIVIL AND WATER ENGINEERING
POLISH ACADEMY OF SCIENCES ISSN 1230-2945

DOI: 10.24425/ace.2022.143040

ARCHIVES OF CIVIL ENGINEERING

Vol. LXVIII ISSUE 4 2022

pp. 311 –330

Research paper

Integration of data obtained from laser scanning and UAV used to develop a 3D model of the building object

Bogusława Kwoczyńska[1], Bogumił Małysa[2]

Abstract: Currently, the possibilities offered by measurement techniques allow development of both cities in the form of 3D models as well as models of small and large architecture objects. Depending on the needs, the scale of an examined object or the intended use of the final product, geodesy finds ready-made measurement methods. If one wants to work out a 3D model of a building object in detail, the most accurate way is to use laser scanning technology. However, there are situations in which limitations resulting from the terrain layout or the structure of the building preclude to obtain full information about its shape. In such situations, the solution is to integrate data from various measurement devices. If creating a full 3D model of large buildings, the best choice to complete data, especially the roof of the object, is to use an unmanned aerial platform, because the resolution of images made on a low altitude is good enough to obtain a satisfactory effect in the form of a point cloud. The research used integration of data obtained at low altitude from two unmanned aerial vehicles, Fly-Tech DJI S1000 and DJI Phantom 3 Advanced – using various types of missions – with data recorded with the Leica ScanStation P40 terrestrial laser scanner. The data was integrated by giving them a common coordinate system – in this case the 2000 system, for the grid points measured in the field with the GNSS technique, and the use of Cyclone, Metashape and Pix4D software for this purpose. Combined point clouds were used for 3D modelling of the sacred object with Bentley CAD software. The accuracy with which data integration was performed and errors resulting from the use of various measurement techniques were determined. The result of the study is a 3D model of the Church of Our Lady of Consolation, located in Krakow at the Sportowe estate.

Keywords: data integration, Terrestrial Laser Skanning, UAV

[1]PhD., Eng., University of Agriculture in Krakow, Faculty of Environmental Engineering and Land Surveying, Al. Mickiewicza 21, 31-120 Krakow, Poland, e-mail: boguslawa.kwoczynska@urk.edu.pl, ORCID: 0000-0001-7230-5397

[2]Eng., RemoteCraftsmen Krakow, ul. Opolska 12, Krakow, Poland, e-mail: bogus1@onet.eu

1. Introduction

Over the last century, the number of measurement methods in geodesy has increased significantly. Along with the increase in techniques for recording land information, accuracy of the instruments collecting this data has also increased. Currently, the possibilities offered by measurement techniques are not limited only to creation of detailed, two-dimensional maps, but also allow development of both cities in the form of 3D models and modelling large and small architecture objects, such as, for example, chapels. Depending on the needs, scale of the examined object (or area), or the intended use of the final product, geodesy finds ready-made measurement methods. For example, if one wants to develop a detailed facade intended, for example, to create technical documentation, the most accurate way is to use a relatively new technology, which is laser scanning. This method gives allows to collect information about the shape and dimensions in the form of a point cloud in a very short time, with remarkable accuracy, where the error often does not exceed tenths of a millimetre. However, there are situations in which limitations resulting from the terrain layout or the structure of the building preclude to obtain full information about its shape. In such situations, the solution is to integrate data from various measurement devices. In such a case, if creating a full 3D model, the best choice to complete data is to use an unmanned aerial platform, because the resolution of images made on a low altitude is good enough to obtain a satisfactory effect in the form of a point cloud [14].

Use of the TLS (Terrestrial Laser Scanning) for the inventory of historic buildings was described, among others by [3, 12, 13, 19, 20]. However, it is common to use integration of photogrammetric and laser data, which is visible in the studies of [5, 11, 16] and [17].

Research on the use of laser scanning for registration and inventory of architectural objects has been conducted for many years all over the world, and the proof are works of [2, 4, 6, 9, 18].

The constant technological progress causes that the old and so far inconvenient methods of collecting geospatial information are replaced by modern technology that has completely revolutionized work of engineers. Such technologies include, among others, laser scanning and data acquisition from UAV (Unmanned Aerial Vehicle).

Unmanned Aerial Vehicle (UAV) has the unique ability to quick exploration of vast area and gathering high-resolution images [15]. According to [22], UAVs have great potential for commercial, scientific and research applications, and the use of professional civilian UAVs around the world is growing rapidly. UAVs help in providing spatial data for civil engineering, mining, GIS, geology, construction and many others [8]. Owing to the almost unlimited possibility of collecting information, UAVs have found a number of applications also in geodesy, cartography, archaeology, cultural heritage, technical and architectural documentation, modelling of buildings, monuments and landscape [7].

The conducted research used integration of data from terrestrial laser scanning and UAV in order to develop a full 3D model of a building object. This integration is based on the use of image data from high-resolution digital cameras and a spatial model obtained from a point cloud. The point cloud obtained from terrestrial laser scanning is supplemented with data from matching, which is the result of automatic image correlation. Integration

of this type of data can be used both in inventory of small objects (single buildings) and large buildings (e.g. churches or building complexes), as well as for inventory of other engineering structures such as slender buildings (chimneys), industrial facilities or even unusual objects such as aeroplanes.

2. Characteristics of the research object

The object subjected to measurement was Our Lady of Consolation Church located in Krakow at the Sportowe estate, at 15a Bulwarowa Street. The construction of the church began on November 3, 2001. The church is a small, modern object with unusual shapes, looking like a fish from the bird's eye view (Fig. 1).

On November 7, 2006, the cornerstone was placed (Fig. 2), previously blessed by the Holy Father John Paul II during his pilgrimage to Poland in 1997.

Fig. 1. Our Lady of Consolation Church in Krakow

Fig. 2. The cornerstone of the Church

3. Data sources

Acquisition of data for 3D modelling and visualization of architectural objects can be done using various measurement techniques. Currently, two techniques that have dominated the services market in terms of inventory can be distinguished. These include photogrammetry, based on high-resolution images, and laser scanning. These methods can be used independently, however, studies have shown that the combination of both techniques is the most effective [3].

The research used integration of low-altitude data from two unmanned aerial platforms: Fly-Tech DJI S1000 and DJI Phantom 3 Advanced – using various types of missions, as well as registration with the Leica ScanStation P40 terrestrial laser scanner.

Selection of two different unmanned flying platforms was due to the fact that each of them separately would not allow to obtain a point cloud fully sufficient for the development of the roof of the facility. Fly-Tech DJI S1000 is equipped with a high-resolution digital SLR

– 36.4 million pixels, but has the ability to perform only a classic mission. Resolution of the camera in which the DJI Phantom 3 Advanced is equipped is lower (12.4 million pixels), but it can perform both classic and elliptical missions, which was especially helpful when registering the lower parts of the roof and walls with stained glass windows. Only the cloud of points, which was created from photos taken from both flying platforms, allowed for the collection of complete information about the roof of the object, as well as its side walls.

3.1. Fly-Tech DJI S1000 unmanned aerial vehicle

DJI S1000 is a professional rotor unmanned aerial vehicle (Fig. 3). It has eight electric motors, 500 W each. Arms and most of its structures are carbon, which results in a low unladen mass (about 4.2 kg) and a stable and compact carrying platform, what is more, the arms and propellers have been designed in such a way that they can be easily folded. A GPS satellite receiver has also been installed, along with the IMU inertial system, which allows to accurately determine its position in space. The power cell is a lithium-polymer battery that provides energy for approximately 15 minutes of flight (with a total weight of 9.5 kg).

Fig. 3. DJI S1000

The eight-rotor is equipped with a full-frame, mirrorless Sony α ILCE 7R camera that gives the opportunity to take pictures with a resolution of just over 36 million pixels, the matrix type is CMOS, giving the opportunity for light measurement in a point, multi-segment or centre-weighted manner. The included lens is a Sony with a focal length of 35 mm and a minimum aperture of $f/1.8$. The bayonet mount is Sony E. The lens has internal stabilization. In addition, its full compatibility with the camera body ensures the use of continuous DMF autofocus [www.cyfrowe.pl].

Additional stabilization of photos taken during the flight is provided by the 3-axis Zenmuse Z15 gimbal. It enables wireless transmission of live image via the HDMI-AV module. It is also equipped with an independent IMU module. The gimbal, in addition to eliminating camera vibrations and tilt, gives the possibility of constant control over the shutter and allows remote control of the camera in three directions.

3.2. DJI Phantom 3 Advanced unmanned aerial vehicle

The Phantom 3 Advanced version (Fig. 4) is a budget four-rotor, used primarily by amateurs of low-altitude flights. Use of components made mostly of plastic results in a weight of 1,280 grams. Lithium-polymer cell provides about 23 minutes of flight thanks to the capacity of 4480 mAh. The image is sent to the screen of a smartphone or tablet in real time, over a maximum distance of about 4–5 kilometres. The DJI product is equipped with a number of sensors: optical, gyroscope, compass, accelerometer, as well as GPS and GLONASS satellite signals receiver, which ensures stable flight and constant position control of the flying platform in the air. The drone has a camera, stabilized with a three-axis gimbal. Its focal length is 20 mm and the minimum aperture value is $f/2.8$. The matrix is a Sony product, marked EXMOR with the size of $1/2.3''$, giving the possibility of taking a photo with a maximum size of 12.4 million pixels and a maximum ISO 1600 value. During a flight, the gimbal allows to control the position of the camera in all three axes, while stabilizing undesirable deflections [14].

Fig. 4. UAV DJI Phantom 3 Advanced

3.3. Leica P40 terrestrial laser scanner

The Leica Geosystems P40 pulsed laser scanner (Fig. 5) was released to the market in 2015. It stands out with its high efficiency of data recording – up to 1 million in one second. The maximum imaging distance is 270 meters. In addition, the geodetic compensator

Fig. 5. Leica P40 scanner

guarantees a low noise level, and what is more, a higher angular accuracy of the acquired data. The scanner has a built-in digital camera, which additionally gives opportunity to register a colour point cloud. Accuracy of coordinates measurement for a single point is 3 mm at a distance of 50 m. The angular accuracy is 8″ in both the vertical and horizontal planes, and the range accuracy is 1.2 mm +10 ppm. The wavelength the scanner uses is 1550nm and 658nm. It is a panoramic type scanner, its field of view is 270° vertically and 360° horizontally. The scanner is powered by two internal and one external hot-swappable lithium-ion battery making possible exchange without interrupting the measurement.

4. Development methodology

As part of the research, it was necessary to perform field measurements (reference network measurement, laser scanning and UAV air raids) as well as officer works, consisting in the processing of data obtained from UAV platforms and terrestrial laser scanning.

4.1. Field work

The field work began with the placement of photopoints around the examined object (Fig. 6) in order to define the reference network, which was then used to integrate all data, both ground and above-ground. 17 photopoints in the form of marks stuck on the ground around the object were selected. Stands with Leica shields, for which heights were measured. were placed above three of the marks. The last stage before proper measurements was the even distribution of reference metal spheres around the object, which gave the opportunity for the subsequent orientation of all clouds obtained with the laser scanner.

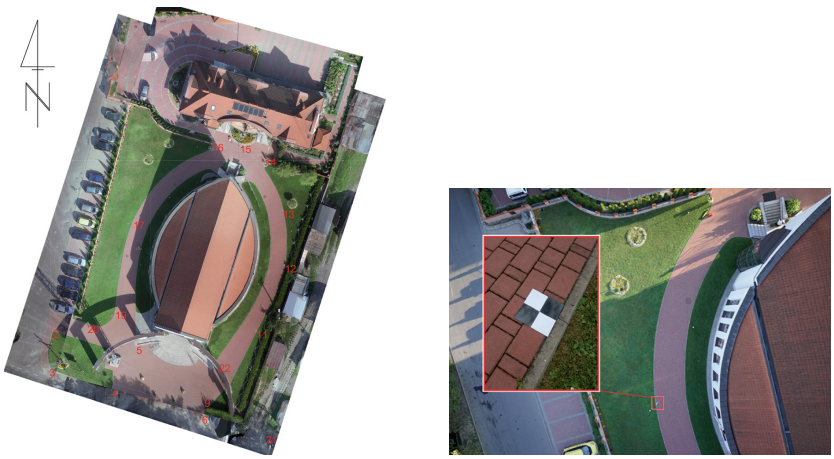

(a) (b)

Fig. 6. Measurement network: a) distribution of photopoints around the object, b) magnification of the selected photopoint

The measurement of the control points was performed with the GNSS Trimble R8-3 receiver, using the GNSS-RTK method (Real Time Kinematic), which involves use of two satellite signal receivers – a static (called the base station) and a mobile one. The base station makes continuous observations, on the basis of which observation corrections are then sent to the dynamic station (e.g. by radio). The ASG-EUPOS continuous measurement system played the role of the base station in the measurement. Control photo points were recorded in the 2000 system.

Information on measurement and mapping parameters is presented in the report in Figure 7.

Receiver manufacturer, model and serial number:	**Trimble, R8-3 5130469013**	Manufacturer and model of the antenna	**Trimble R8 GNSS/SPS88x Internal**
Use of the ASG-EUPOS system:	**Yes**	User name to access the ASG-EUPOS system:	–
Type of corrections used:	**VRS_RTCM_3_1**	ASG-EUPOS corrections stream used:	**RTCM 3.2**
IP address:, IP port:	**http://178.73.5.200: 2101**	Raw Observation Record:	**No**
Rover Receiver Elevation Mask:	**10**	Rover Receiver PDOP Mask:	**6**
Date of first measured point:	**18 September 2018**	Date of last measured point:	**18 September 2018**
Firmware Type:	**Trimble General Survey**	Firmware version:	**2.50**

Mapping parameters:

Country Layout / zone Reference ellipsoid	Poland 2000/21 WGS-84
Large semiaxis of the ellipsoid Flattening of the ellipsoid	6378137 0.00335281067183
Mapping type Axial parallel Axial meridian Principal point X Principal point Y Scale at the main point Azimuth Grid orientation	Transverse Mercator 0 21 0 7500000 0.999923 To the north Ascending north-east
Altitude transformation Geoid model	Geoid plervf07

Fig. 7. Information on measurement and mapping parameters

Full measurement report shows that the error in determining XY coordinates of photopoints did not exceed 6 mm, while the error in determining Z coordinate did not exceed 11 mm.

4.2. UAV raids

One of the methods of measuring buildings is the use of an unmanned aerial vehicle (UAV) serving as a carrier for a device enabling the use of photogrammetric technology. Unmanned Aerial Vehicle (UAV) is a breakthrough in science and technology. It has the unique ability to quickly explore vast area and acquire high-resolution images [15]. It makes a real and cheap alternative to air and space sensors used for medium and large scale object mapping [1].

In order to develop a 3D model of the tested object, various types of missions were carried out as part of the UAV raids – classic ones to obtain images from the aerial altitude, and elliptical ones.

4.2.1. Raid using Fly-Tech DJI S1000 UAV

During the DJI S1000 drone raid, the flight altitude was 50 m above ground level. In total, imaging was made in three rows, and the mission time was 13 minutes. During the flight, 17 high-resolution photo images were recorded. Moreover, in addition to the photos necessary for the subsequent generation of the point cloud, photos of the stained glass windows were also taken to be used for texturing the model (Fig. 8). The exposure time of each photo was fixed at 1/1000 s, which resulted in a slight blur. Sensitivity of the ISO matrix has also been set to a fixed value of 800. So the exposure value was manipulated by automatic change of closing and opening of the aperture of the camera, where the largest opening was $f/2.8$ and the largest closing was $f/4.5$.

Fig. 8. Photo of the stained glass made for the purpose of texturing the 3D model

4.2.2. Air raid with DJI Phantom 3 Advanced UAV

The raid with the Phantom 3 drone was possible thanks to the Pix4D software. The Pix4Dcapture module, which is also an application adapted to Android, was used to programming the mission. This program allows to choose several mission variants. Ultimately,

two types have been selected – *grid mission*, which is a traditional type of aerial imagery, and *circular mission*, which consists in making a circle or ellipse around a selected object, while taking pictures at a high angle, which allows getting a better view of the terrain, as well as complementing information gaps of traditional mission.

The flight altitude was defined at 35 meters above ground level for the 3D mission and 50 meters for the traditional raid, and the flight path was set for each mission. For the 3D mission, the pixel size was 2.66 cm, while, for the *grid mission* it was about 2.16 cm. In total, 43 photos were taken in the elliptical mission and 23 in the traditional one.

After completing two missions, the photos were exported from the UAV to the smartphone, and then, after connecting to the Internet, sent to the cloud, to the server of the Pix4D software producers. The pictures were processed there to be available for download as an entire project, along with an orthophotomap, point cloud, detailed report and many other products.

4.3. Field measurement with the Leica P40 laser scanner

Terrestrial laser scanners (TLS) are actually electronic total stations that perform a reflectorless distance measurement. The basic model of a terrestrial laser scanner consists of a transmitter, rotating mirrors, an optical telescope, a detector and a recorder. The transmitter produces a laser beam that reaches a system of rotating mirrors [21]. Owing to this, it is precisely distributed over the surface of the object with an appropriate resolution, which in turn leads to the acquisition of a point cloud.

Measurements with the Leica ScanStation P40 laser scanner started after setting the appropriate vertical and horizontal scanning resolution to 2 mm. The option of photographic images with the internal camera was also turned on so that the cloud finally contained information about the RGB values of individual points. In total, data was recorded for 15 stations. During the measurements at subsequent stations, efforts were made to limit the angular range of the scanner's rotation to exclude those areas that were not provided for the later study, and thus reducing the total time of work performed and the volume of files, but in such a way that provides capture of as many reference balls as possible in the frame.

4.4. Generating point clouds from photos

The office works consisted of integration of data obtained with two aircraft and a laser scanner by assigning them common georeferencing, based on the measured reference grid using the GNSS method, which gave the basis for development of a 3D model of the sacred object.

Agisoft's Metashape software made it possible to orientate photos by registering control points with markers on each photo. However, before that, a file containing the coordinates of the photopoints in the 2000 system, which were intended by the GNSS technique had to be loaded.

A total of 83 images were used:

– 43 photos that were recorded with the Phantom 3 Advanced drone in the 3D mission,

– 23 photos, also captured with the Phantom 3 in the classic raid,
– 17 photos taken with the DJI S1000 drone in a traditional mission.

After the mutual orientation of the photos, the mean error was 4.7 cm and it was within the acceptable values. Next, a point cloud, representing the church along with the nearby area, was generated (Fig. 9), with real georeferencing, which was exported to the .las format.

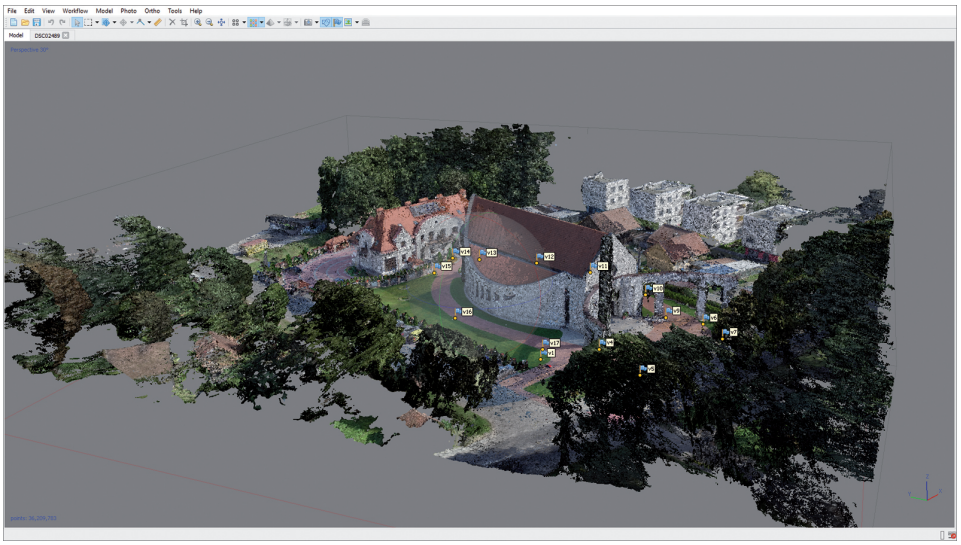

Fig. 9. Point cloud generated in the Metashape environment

4.5. Integration of point clouds from photos and laser scanning

Work related to the mutual orientation of all point clouds measured with a laser scanner was limited to registration of reference spheres and points indicated with discs. The orientation of the point clouds from the ground scanning was done in the Leica Cyclon software, achieving an average error of 3 mm.

The final part of the work in the Cyclone environment was integration of point clouds obtained from photos and laser scanning. It required importing a point cloud in the .las format (previously acquired in Metashape), generated on the basis of photos from the raids. Due to the previously assigned georeferencing, the point cloud coincided with the point clouds from laser scanning, to which they were also assigned in the previous stage. Inaccuracy of the coverage that the clouds were burdened with was determined manually by 10 times measurement of the distance between the same points for both the ground and the roof slopes in various places (Table 1), and then averaging the obtained values. Points were selected on each side of the building, both in its highest parts (around the ridge), in the lower parts of the roof, and on the ground around the building. The results obtained were 49.8 mm of non-compliance on the roof and 23.8 mm on the ground, so the mean

error was 36.8 mm. It should be noted, however, that the determination of these errors is not an exact representation of the actual shifts, but is only an approximate representation of the inaccuracy value of coverages between clouds.

Table 1. Compilation of the results of measuring incompatibility between point clouds

No.	Measurement on the roof [m]	Measurement on the ground [m]
1	0.0279	0.0323
2	0.0336	0.0217
3	0.0279	0.0244
4	0.0258	0.0336
5	0.0786	0.0290
6	0.0550	0.0191
7	0.0945	0.0146
8	0.0478	0.0256
9	0.0408	0.0173
10	0.0663	0.0208
Average:	**0.0498**	**0.0238**

In order to assess the accuracy of the integrated point clouds, and as a result of the obtained object model, the distances between the photopoints and the characteristic points of the object (Table 2), the distances between the photopoints (Table 3) and the distances inside the point clouds (Table 4) obtained on the basis of TLS and UAV measurements. In case of special points of the object, they were selected both in the upper parts of the object (roof), in its middle and lower parts. Distances inside the point clouds were also selected within the entire facility and measured in horizontal and vertical directions, and the sections are of different lengths (the maximum for the ridge is over 36 m). An example of the distribution of the measured distances is shown in Figure 10. The distances are shown in different colours, where the distances between the photopoints are shown in blue, the distances between the photopoints and the characteristic points of the object in red, and the distances inside the point clouds in yellow.

When analysing the obtained results, it should be noted that the greatest differences in the measurements of the distances between photopoints and the characteristic points of the object, obtained on the basis of TLS and UAV measurements, occur when the characteristic points are located in the upper parts of the object (on the roof). The greatest value of the difference in measurements to the point located on the ridge was 0.147 m, while the minimum value for points in the lower parts of the structure was 0.02 m. The average value for all measured sections was 0.076 m.

Table 2. Summary of distances between photopoints and characteristic points on the basis of TLS and UAV measurements

No.	Photopoint	Characteristic pointe of the object	Distance based on UAV [m]	Distance based on TLS [m]	Difference from TLS and UAV measurements [m]
1	FT17	1	26.223	26.250	0.027
2	FT17	3	10.551	10.698	0.147
3	FT16	4	18.822	18.933	0.111
4	FT16	3	19.062	19.156	0.094
5	FT19	2	9.440	9.460	0.020
6	FT5	5	19.850	19.889	0.039
7	FT5	6	18.260	18.381	0.121
8	FT11	7	14.468	14.474	0.006
9	FT12	8	10.087	10.184	0.097
10	FT13	9	13.144	13.244	0.100
11	FT13	10	12.150	12.215	0.065
12	FT13	4	22.010	22.096	0.086
				Average	**0.076**

Table 3. Summary of distances between photopoints obtained on the basis of TLS. UAV and RTK measurements

No.	Photopoint No.	Distance based on RTK [m]	Distance based on UAV [m]	Distance based on TLS [m]	Difference from TLS and UAV measurements [m]	Difference from TLS and RTK measurements [m]	Difference from UAV and RTK measurements [m]
1	FT16- FT14	12.444	12.445	12.461	0.016	0.017	0.001
2	FT17- FT16	25.252	25.312	25.319	0.007	0.067	0.060
3	FT19- FT17	20.955	20.937	20.963	0.026	0.008	–0.018
4	FT5- FT19	9.34	9.319	9.357	0.038	0.017	–0.021
5	FT5- FT4	11.295	11.271	11.288	0.017	–0.007	–0.024
6	FT22- FT11	11.503	11.531	11.533	0.002	0.030	0.028
7	FT11- FT12	16.344	16.269	16.313	0.044	–0.031	–0.075
8	FT12- FT13	12.416	12.476	12.477	0.001	0.061	0.060
9	FT13- FT14	12.558	12.524	12.526	0.002	–0.032	–0.034
10	FT6- FT22	12.403	12.359	12.419	0.06	0.016	–0.044
				Average	**0.021**	**0.015**	**-0.007**

Table 4. Summary of distances inside point clouds obtained from TLS and UAV measurements

No.	Starting point	End point	Distance based on UAV [m]	Distance based on TLS [m]	Difference from TLS and UAV measurements [m]
1	1	2	36.334	36.495	0.161
2	3	4	3.928	4.033	0.105
3	5	6	27.506	27.551	0.045
4	7	8	8.672	8.764	0.092
5	9	10	3.476	3.560	0.084
6	11	12	9.243	9.201	–0.042
7	13	14	11.433	11.585	0.152
8	15	16	9.412	9.322	–0.090
9	17	18	8.762	8.771	0.009
10	19	20	7.332	7.480	0.148
				Average	**0.066**

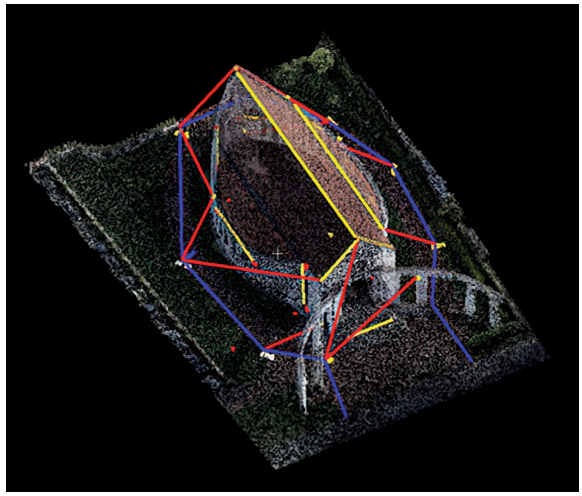

Fig. 10. An example of the distribution of the measured distances on the tested object (blue – distances between photopoints, red – distances between photopoint and characteristic point, yellow – distances inside the point cloud)

A similar situation occurs in case of sections measured inside the point clouds obtained from TLS and UAV, and placed on the roof (for the ridge the maximum difference was 0.161 m), while for the sections measured in its lower parts the minimum value was 0.009 m. Average value for all measured distances was 0.066 m.

In the case of the distance between photopoints measured on the point clouds from TLS and UAV measurements, the mean value of the difference was 0.021 m. These distances were compared with the results obtained from RTK measurements for each of the methods separately. The average values of the differences did not exceed 0.02 m (0.015 m for TLS and –0.007 m for UAV).

4.5.1. Point clouds cleaning and limiting them to the scope of the object

After the point cloud was integrated and oriented, it was necessary to limit the scope of all clouds to the required area of study, and then to clean them from noise and elements obscuring the image, such as, for example, passing pedestrians captured in the scanner frame.

The process of limiting and cleaning the point cloud reduces the use of computer components in later study, which gives greater freedom of operation. Carrying out the above processes led to a ready representation of the object in the form of a point cloud shown in Figure 11.

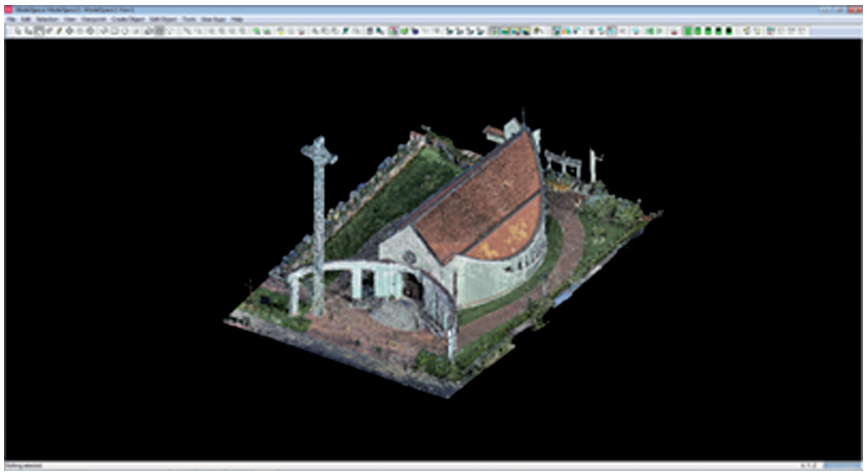

Fig. 11. Point cloud in real RGB colours after necessary treatments

5. 3D modelling of a building object based on integrated data

The process of 3D modelling comes down to creating a three-dimensional object with the use of specialized computer software, which most often provides ready-made tools, e.g. in the form of basic geometric figures [www.wikipedia.org/wiki/Modelowanie_(3D)].

According to [3], one of the most accurate data sources about an object is a point cloud, which can be obtained using a dedicated instrument – a laser scanner, or generated on the basis of photogrammetric studies and stereoimages.

Ready-made 3D models of architectural objects are used in many aspects of life. They can be used, for example, to determine the degree of sunlight and shade, they are extremely helpful in creating acoustic maps using simulations of noise sources. Simulation can also be used to analyse and then prevent potential threats such as flooding, fires or strong winds in crisis management. 3D models of buildings are often used by developers to better present their housing offers through animation and visualization. Advanced CAD systems (Computer Assisted Design) / CAM (Computer Assisted Manufacturing), in addition to the standard possibility of creating 3D models, have the option of giving them physical properties of real objects, which allows to perform engineering calculations on the model and to perform kinematic and dynamics analysis of individual elements and their entire components, which results in the possibility of testing on the model such features as, e.g. deformation strength, temperature resistance, or even the maximum load capacity [3, 10].

As part of the research, the last and final stage of the office works was creation of a 3D model of the church based on a previously prepared point cloud. This process was performed in a CAD program, ie Bentley's MicroStation V8i. Previously, however, exporting point clouds from the Cyclone program to separate files made it possible to load each cloud registered at a given position on a separate layer. It was an important aspect from the point of view of the comfort of work during modelling, because – in the case of using a workstation and insufficient amount of RAM – it gives an opportunity to work only on the necessary part of the point cloud by switching off layers with selected clouds.

The modelling process was started by creating the outline of the church body, based on the cross-section of point clouds (Fig. 12). Most of the elements were created in a similar way. By cutting the appropriate profile along the walls, it was possible to draw their outline, and then to draw more solids using an appropriate tool.

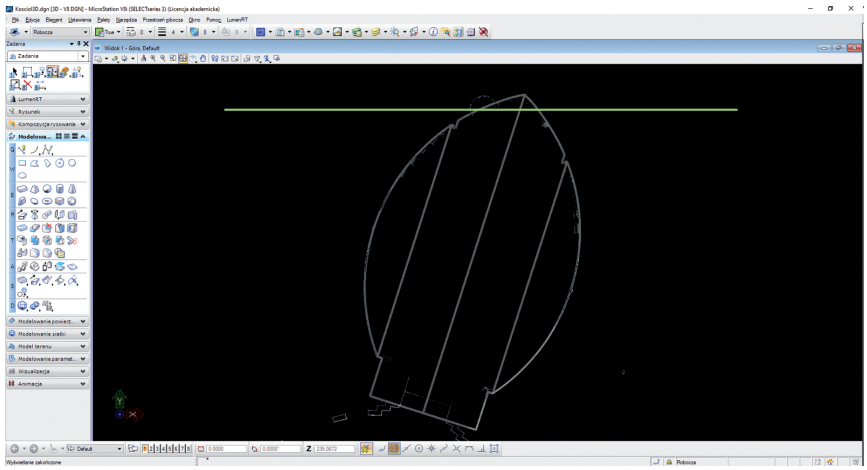

Fig. 12. The outline of the object on the external walls – top view

Having the most important shapes, such as the roof or the main body of the church, they had to be detailed. In the case of the main body, e.g. by cutting out windows (Fig. 13).

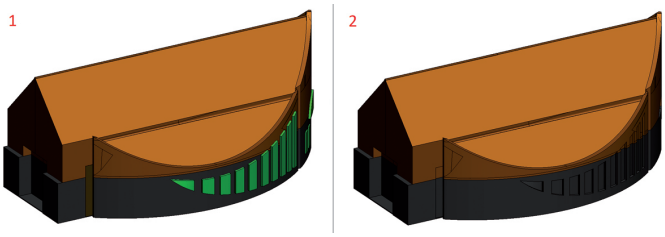

Fig. 13. The solid model of the object: 1 – model before cutting out the windows, 2 – model after cutting out the windows

More complicated surfaces, such as arches on the roof or arches in front of the church, were created in two stages. Use of appropriate MicroStation tools made it possible to create a skeleton model first, and then a solid model of the church. Finally, a 3D model of the church at Bulwarowa Street in Krakow, shown in Figure 14, was obtained, but without any textures.

The last stage of work, in order to make the model look real, was to cover each element with an appropriate texture. Most of the textures were made by taking photographs of all the elements in the field and then cutting out specific areas from them. The final result is an isometric projection model shown in Figure 15.

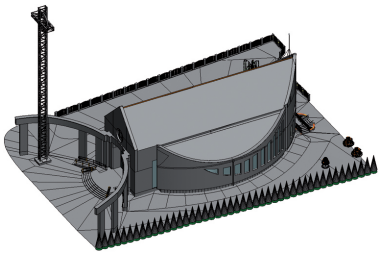

Fig. 14. Ready 3D model without textures

Fig. 15. 3D model with superimposed

Figures 16–19 show the model of the church in side, front and rear views.

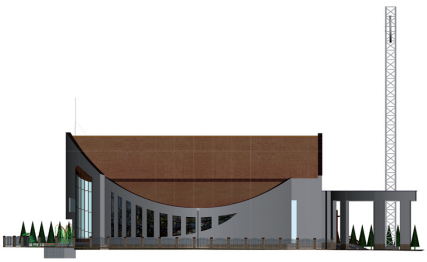

Fig. 16. 3D model in the left-side view

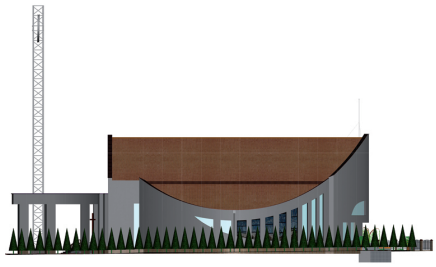

Fig. 17. 3D model in the right-side

Fig. 18. 3D model in front view

Fig. 19. 3D model in rear view

6. Conclusions

Data integration, despite their many sources, was so successful that basing on the point clouds oriented in the 2000 system, it was possible to create the model presented above. What's more, it is worth noting that the data obtained by the use of a laser scanner are characterized by greater accuracy (average orientation error equal to 3 mm), compared to the point cloud generated on the basis of photos taken in a total of three missions with two flying platforms (average error of cloud fitting – 24 mm). However, during the modelling process, the points representing individual elements located in the field reflected their real surfaces so well that during modelling no problems with the interpretation of the given fragments of objects were found [14].

The presented example of data integration has shown that the two methods of obtaining data (TLS and UAV) can complement each other in creating high-resolution 3D studies. Three-dimensional point cloud obtained from laser scanning is used to create high-resolution geometric models, while the UAV provides high-resolution images, allowing to supplement the data obtained by scanning.

On the basis of additional measurements of distance on point clouds from TLS and UAV measurements, it can be concluded that the accuracy of the church model made on the basis of integrated point clouds is within 0.10 m. The greatest discrepancies in point clouds occurred in the upper parts of the roof, which It is characterized by a large slope (roof deflection is 12 m), and they amounted to a maximum of 0.16 m. The differences in the lower part of the structure were within 0.02 m.

Based on the research, the following conclusions can be drawn:

– Structure of the facility often makes it impossible to use only one measuring instrument in order to obtain complete information about the building. Such an example is a church, the model of which was created as a result of the integration of TLS and UAV data. Using only TLS data would not allow for a complete and accurate mapping of the roof of the building with a very characteristic shape.
– Detailed modelling of architectural objects based on a point cloud is a very laborious process, but it allows to develop an object in a very accurate way. This labour

consumption depends mainly on the scale of accuracy and the visual effect you want to achieve, and this mainly applies to the reproduction of small details most often occurring on the facade of the building. In the case of the presented church, it was also important to map the stained glass windows on the side walls of the building, which required taking additional photos with a DSLR and fitting them into the oval walls of the church.

– Use of aerial methods, such as low-altitude imaging of UAVs, turns out to be a good choice to supplement information, for example, on roof slopes – places that are difficult to reach using only TLS.
– Integration of data in a common coordinate system enables full visualization and insight into the architecture of the examined object.
– Accuracy of the object model created from TLS and UAV data integration strictly depends on the accuracy of point cloud integration, in the case of the presented object it varied within 10 cm.
– By using the CAD program environment and tools, the user is able to create an almost identical digital copy, which in turn allows the creation of complete documentation, and may also be helpful in any conservation works.
– An additional advantage of the model made in the CAD environment is the possibility of animating such a model of a building object.

Acknowledgements

Financed by a subsidy from the Ministry of Education and Science for the University of Agriculture im. Hugona Kołłątaja in Krakow for 2022.

References

[1] R. Al-Tahir, "Integrating UAV into Geomatics Curriculum", in *ISPRS International Archives of the Photogrammetry, Remote Sensing and Spatial Information Sciences*. 2015, vol. XL-1-W4, pp. 387–390.

[2] M. Bernat, A. Janowski, S. Rzepa, "Studies on the use of terrestrial laser scanning in the maintenance of buildings belonging to the cultural heritage", *14th SGEM GeoConference on Informatics, Geoinformatics and Remote Sensing*, 2014, vol. 3, pp. 307–318; DOI: 10.5593/sgem2014/b23/s10.039.

[3] K. Michałowska, Ed., *Modelowanie i wizualizacja danych 3D na podstawie pomiarów fotogrametrycznych i skaningu laserowego*. Rzeszów: WSIE, 2015, ISBN 978-83-60507-29-2.

[4] W. Boehler, A. Marbs, "3D Scanning and Photogrammetry for Heritage Recording: a Comparision", in: *Proceedings of the 12th International Conference of Geoinformatics*. Gavle University Press, 2004, ISBN: 91-974948-1-X, pp. 291–298.

[5] S.J. Buckley, J.A. Howell, H.D. Enge, B.L.S. Leren, T.H. Kurz, "Integration of Terrestrial Laser Scanning, Digital Photogrammetry and Geostatical Methods for High-Resolution Modelling of Geological Outcrops", in *The International Archives of the Photogrammetry, Remote Sensing and Spatial Information Sciences*, vol. 36, part B. Dresden, Germany, 2006.

[6] R. Cantoni, G. Vassena, C. Lanzi, "Laser Scanning and Traditional Survey Integration to Build a Complete 3D Digital Model of Sagrestia dell'Archivo di Stato a Mantova", in *Proc. CIPA-ISPRS Workshop on Scanning for Cultural Heritage Recording, Korfu, Greece 2002*. 2002, pp. 105–114.

[7] H. Eisenbeiss, M. Sauerbier, "Investigation of UAV systems and flight modes for photogrammetric applications", *Photogrammetric Record,* 2011, vol. 26, no. 136, pp. 400–421; DOI: 10.1111/j.1477-9730.2011.00657.x.

[8] N.M. Figueira, I.L. Freire, O. Trindade, E. Simoes, "Mission-oriented sensor arrays and UAVs; a case study on environmental monitoring", in: *ISPRS International Archives of the Photogrammetry, Remote Sensing and Spatial Information Sciences*. 2015, vol. XL-1/W4, pp. 305–312; DOI: 10.5194/isprsarchives-XL-1-W4-1-2015.

[9] S. Mikrut, E. Głowienka, Eds., *Fotogrametria i skaning laserowy w modelowaniu 3D*. Rzeszów: WSIE, 2015, ISBN 978-83-60507-26-1.

[10] T. Gorecki, P. Penkała, "Modelowanie bryłowe i powierzchniowe w systemach CAD/CAM", *Postępy Nauki i Techniki*, 2010, no. 4, pp. 75–84.

[11] A. Guarnieri, F. Remondino, A. Vettore, "Digital Photogrammetry and TLS Data Fusion Applied to Cultural Heritage 3D Modelling", in *The International Archives of the Photogrammetry, Remote Sensing and Spatial Information Sciences*, vol. 36, part B. Dresden, Germany, 2006.

[12] M. Kędzierski, P. Walczykowski, A. Fryśkowska, "The monthly geoinformation Laser Scanners appendix", *Appendix Geodeta Magazine, Scanning Monuments*, 2008, pp. 36–38.

[13] B. Kwoczyńska, U. Litwin, P. Obirek, I. Piech, J. Śledź, "The Use of Terrestrial Laser Scanning in Surveying Historic Buildings", *IEEE Xplore,* 2016, pp. 263–268; DOI: 10.1109/BGC.Geomatics.2016.54.

[14] B. Małysa, "Integracja danych z UAV i naziemnego skaningu laserowego wykorzystana w opracowaniu modelu 3D obiektu sakralnego", M.A. thesis, Uniwersytet Rolniczy w Krakowie, 2019.

[15] A.J.S. McGonigle, A. Aiuppa, G. Giudice, G. Tamburello, A.J. Hodson, S. Gurrieri, "Unmanned aerial vehicle measurements of volcanic carbon dioxide fluxes", *Geophysical Research Letters,* 2008, vol. 35, no. 6; DOI: 10.1029/2007GL032508.

[16] S. Mikrut, A. Moskal, U. Marmol, "Integration of image and laser scanning data on selected example", *Image Processing & Communication*, 2014, vol. 19, no. 2-3, pp. 37–44.

[17] B. Mitka, A. Rzonca, "Integration of photogrammetric and 3D laser scanning data as a flexible and effective approach for heritage documentation", presented at 3rd ISPRS International Workshop 3D-ARCH, 2012.

[18] K. Pyka, A. Rzonca, "Badanie jakości radiometrycznej ortofotogramów sporządzonych na drodze integracji fotogrametrii biskiego zasięgu i skaningu", *Archiwum Fotogrametrii, Kartografii i Teledetekcji*, 2006, vol. 16, pp. 512–526.

[19] F. Remondino, S. El-Hakim, S. Girardi, et al., "3D Virtual Reconstruction and Visualization of Complex Architectures", *International Archives of Photogrammetry, Remote Sensing and Spatial Information Sciences*, 2009, vol. XXXVIII-5/W1, pp. 1–9.

[20] A. Rizzi, F. Voltolini, F. Remondino, S. Girardi, "Heritage recording and 3D modeling with photogrammetry and 3D scanning", *Remote Sensing*, 2011, vol. 3, no. 6, pp. 1104–1138; DOI: 10.3390/rs3061104.

[21] M.S. Quintero, J.L.L. Garcia, B.V. Genechten, *3D Risk Mapping Theory and Practice on Terrestrial Laser Scanning*. *Training Material Based on Practical Applications*. Universidad Politecnica de Valencia, Spain, 2008.

[22] A. Wójcik, P. Klapa, B. Mitka, I. Piech, "The use of TLS and UAV methods for measurement of the repose angle of granular materials in terrain conditions", *Measurement,* 2019, vol. 146, pp. 780–791; DOI: 10.1016/j.measurement.2019.07.015.

[23] [Online]. Available: https://pl.wikipedia.org/wiki/Modelowanie_(3D).

[24] [Online]. Available: https://www.cyfrowe.pl/.

Integracja danych pozyskanych ze skaningu laserowego oraz UAV wykorzystana do opracowania modelu 3D obiektu budowlanego

Słowa kluczowe: naziemny skaning laserowy, UAV, integracja danych

Streszczenie:

Obecnie możliwości jakie dają techniki pomiarowe, pozwalają na opracowywanie zarówno miast w postaci modeli 3D, jak i modeli obiektów małej i dużej architektury. W zależności od potrzeb, skali badanego obiektu, czy przeznaczenia finalnego produktu, geodezja znajduje gotowe metody pomiarowe. Chcąc szczegółowo opracować model 3D obiektu budowlanego, najdokładniejszym sposobem okazuje się wykorzystanie technologii skaningu laserowego. Jednak są sytuacje, w których ograniczenia wynikające z układu terenowego lub konstrukcji budynku, nie pozwalają na pozyskanie pełnej informacji o jego bryle. W takich sytuacjach rozwiązaniem jest zintegrowanie danych z różnych sprzętów pomiarowych. W przypadku tworzenia pełnego modelu 3D dużych obiektów budowlanych, najlepszym wyborem do uzupełnienia danych, szczególnie dachu obiektu, jest użycie bezzałogowej platformy latającej, gdyż rozdzielczość zobrazowań wykonanych na niskim pułapie jest na tyle dobra, że pozwala otrzymać zadowalający efekt w postaci chmury punktów. W badaniach wykorzystano integrację danych pozyskanych z niskiego pułapu z dwóch bezzałogowych platform latających, Fly-Tech DJI S1000 i DJI Phantom 3 Advanced – wykorzystując różnego rodzaju misje – z danymi zarejestrowanymi naziemnym skanerem laserowym Leica ScanStation P40. Zintegrowanie danych obyło się poprzez nadanie im wspólnego układu współrzędnych – w tym przypadku układu 2000, dla pomierzonych w terenie techniką GNSS punktów osnowy oraz wykorzystanie do tego celu oprogramowania Cyclone, Metashape i Pix4D. Połączone chmury punktów wykorzystano na cele modelowania 3D obiektu sakralnego w oprogramowaniu CAD firmy Bentley. Określono dokładność, z jaką przebiegła integracja danych oraz błędy wynikające z zastosowania różnych technik pomiarowych. Efektem opracowania jest model 3D Kościoła Matki Bożej Pocieszenia, znajdującego się w Krakowie na osiedlu Sportowym.

Received: 2022-03-25, Revised: 2022-04-29